Ribosomal protein RACK1 facilitates efficient translation of poliovirus and other viral IRESs

Ethan LaFontaine*[1], Clare M. Miller*[1], Natasha Permaul[1], Alex G. Johnson[2], Elliot T. Martin[1], Gabriele Fuchs[1,3]

* These authors contributed equally to this work

[1] Department of Biological Sciences, University at Albany, Albany, NY, 12222

[2] Department of Chemical and Systems Biology, Stanford University, Stanford, CA, 94305

[3] The RNA Institute, University at Albany, NY, 12222

Abstract

Viruses have evolved various strategies to ensure efficient translation using host cell ribosomes and translation factors. In addition to cleaving translation initiation factors required for host cell translation, poliovirus (PV) uses an internal ribosome entry site (IRES) to bypass the need for these translation initiation factors. Recent studies also suggest that viruses have evolved to exploit specific ribosomal proteins to enhance translation of their viral proteins. The ribosomal protein receptor for activated C kinase 1 (RACK1), a protein of the 40S ribosomal subunit, was previously shown to mediate translation of the 5′ cricket paralysis virus and hepatitis C virus IRESs. Here we found that while translation of a PV dual-luciferase reporter shows only a moderate dependence on RACK1, PV translation in the context of a viral infection is drastically reduced. We observed significantly reduced poliovirus plaque size and a delayed host cell translational shut-off suggesting that loss of RACK1 increases the length of the virus life cycle. Our findings further illustrate the involvement of the cellular translational machinery in PV infection and how viruses usurp the function of specific ribosomal proteins.

Introduction

Since viruses rely on cellular translation factors and ribosomes for translation of viral proteins, viruses and host cells battle for these critical resources. Viral double-stranded RNA activates interferon-induced, double-stranded RNA-activated protein kinase (PKR), which phosphorylates translation initiation factor eIF2α leading to inhibition of viral and cellular translation (1–3). To prevent eIF2α phosphorylation and translational shut-off, viruses target PKR. Some viral proteins directly bind to PKR to prevent its activity, other viruses degrade PKR or alter its subcellular localization (4–9). To efficiently compete for ribosomes, many viruses use translation initiation mechanisms distinct from cellular mRNA translation initiation, which uses canonical cap-dependent translation. All cellular mRNAs are transcribed in the nucleus, where they are also capped and polyadenylated. After export into the cytoplasm, the 5′ m^7GpppN cap is bound by the cap binding protein eukaryotic initiation factor 4E (eIF4E) and the polyA-tail is bound by the polyA binding protein (PABP). Through binding of the scaffolding protein eIF4G to eIF4E and PABP, the mRNA is circularized. With help of the RNA helicase eIF4A, the 40S ribosomal subunit in complex with eIF2 and eIF3 scans the 5′ untranslated region (UTR) in an ATP-dependent manner until the start codon is reached and recognized. After 60S ribosomal subunit joining and GTP hydrolysis by eIF5B elongation can proceed. To prevent cap-dependent translation poliovirus (PV) and other viruses of the *Picornaviridae* family target these eIFs. Specifically, PV proteases 2A and 3C cleave eIF4G, and PABP and eIF5B, respectively (10–16). Cleavage of these essential translation factors

shuts-off host cell translation, while PV uses an internal ribosome entry site (IRES) for translation of the viral polyprotein that does not rely on these translation factors (16, 17). Viruses not only prevent global translation inhibition in the host cell, they also employ strategies that specifically decrease translation of cellular mRNAs.

In addition to targeting translation initiation factors, several viruses have shown direct usage of ribosomal proteins to increase their viral translation. Lee et al. performed an siRNA screen and identified eight ribosomal proteins including eL40, that are not required for cell viability, but negatively affect Vesicular Stomatitis Virus (VSV) and other related viruses (18). Ribosomal protein eL40 was dispensable for viruses that use IRES-mediated translation, but regulated a subset of cellular mRNAs with diverse functions (18). In contrast to eL40, eS25, a protein located near the head of the 40S ribosomal subunit, mediates translation of viruses that initiate translation using IRESs (19, 20). eS25 directly interacts with the hepatitis C virus (HCV) and the intergenic (IGR) cricket paralysis virus (CrPV) IRESs in cryo-EM structures (21–24) and is required for high-affinity binding of the 40S ribosomal subunit to the CrPV IRES (19). Further, eS25 not only facilitates translation of other IRESs such as encephalomyocarditis virus (EMCV) and PV, but also regulates translation of cellular IRES-containing mRNAs (20). More recently, another ribosomal protein, receptor for activated C kinase 1 (RACK1) has been shown to be exploited by different viruses.

RACK1 is a core ribosomal protein (25) that belongs to the tryptophan-aspartate repeat (WD-repeat) protein family. The seven-bladed β-propeller structure of

RACK1 is located near the mRNA exit tunnel where it makes contacts with the ribosomal RNA through lysine and arginine residues and neighboring ribosomal proteins (26–28). RACK1 is often termed a scaffolding protein and has been implicated in a variety of biological function on and off the ribosome. In addition to binding to its eponym protein kinase C βII (PKCβII) and being involved in cellular signaling via Src protein-tyrosine kinase (29–31), RACK1 has been shown to interact with the microRNA machinery (32), bind eIF6 to regulate the 60S ribosomal subunit (33) and regulate ribosome-associated quality control (34, 35). At the level of tissues and organisms, RACK1 regulates axonal growth (36), neural tube closure in *Xenopus laevis* (37), and is essential for development in mice (38), *Drosophila melanogaster* (39) and *Arabidopsis thaliana* (40, 41), but appears to be dispensable in single cell organisms such as yeast (27). Directly and/or indirectly, RACK1 also influences translation of cellular mRNAs. The *Saccharomyces cerevisiae* RACK1 homolog, Asc1, facilitates efficient translation of mRNAs containing a short open reading frame (42), while in mammalian cells, RACK1 appears to stimulate cell proliferation in a PKCβII-dependent manner (30, 43, 44).

At the intersection of cellular signaling and translational regulation, RACK1 represents a critical regulatory target for many viruses. Vaccinia virus, which belongs to the poxviruses and contains a dsDNA genome, but replicates exclusively in the cytoplasm, encodes a kinase that phosphorylates a flexible loop in RACK1 (45). Through phosphorylation, this RACK1 loop is now negatively charged, which allows for translation of the poxvirus polyA-leader

containing mRNAs (45). In plants, where polyA-leader sequences are commonly found, this RACK1 loop contains several glutamic acid residues, hence poxvirus evolution likely rediscovered efficient translation of polyA-leaders through phosphorylation of RACK1. Viruses from the *Dicistroviridae* family encode two polyproteins, and translation of each polyprotein is mediated by an IRES (46). In contrast to eS25, RACK1 is dispensable for translation of the CrPV IGR IRES, but its loss inhibits the translation of both the 5′ IRES of CrPV as well as the HCV IRES (47).

The finding that RACK1 facilitates efficient translation of the HCV IRES prompted us to explore if the need for RACK1 is more broadly conserved. Using a RACK1 knockout cell line generated by CRISPR-Cas9 genome editing (45), we first tested translation using dual-luciferase constructs. We found that HCV, EMCV and PV IRES translation are all reduced in cells lacking RACK1. Although the effect on PV translation in the context of the dual-luciferase reporter is moderate, loss of RACK1 causes a significant decrease in the PV plaque size. This decrease is due to attenuated translation prior to and post translational shut-off, suggesting that the virus life cycle lengthened in cells lacking RACK1.

Results

RACK1-FLAG is incorporated into polysomes

To investigate the function of mammalian RACK1 in translation, we established a functional rescue by expressing RACK1-FLAG in HAP1-derived CRISPR genome edited RACK1 knockout cell line RACK1 KO #1 described by Jha et al.

(45) using lentiviral transduction (48). HAP1 cells are a near-haploid human cell line derived from chronic myelogenous leukemia KBM-7 cells (49). RACK1 was undetectable in RACK1 KO #1 and RACK1 KO #2 cell lines. Following lentiviral transduction of RACK1-FLAG into RACK1 KO #1 cells, RACK1 levels were partially restored (figure 1A). To examine incorporation of FLAG-tagged RACK1 into translating ribosomes rather than other high molecular weight cytosolic complexes, we performed polysome analysis by sucrose gradient ultracentrifugation. When cell lysate is treated with the translation elongation inhibitor cycloheximide, translation will be stalled. Upon sucrose gradient ultracentrifugation, the translating ribosomes, polysomes, are separated from the ribosomal subunits. When sucrose gradient analysis was performed on wildtype HAP1 and RACK1-FLAG expressing RACK1 KO #1 cells, no major differences in the overall polysome profile were detected (figures 1B and 1C).

We found that RACK1-FLAG co-sedimented in the polysomal fractions 9-14 (figure 1C, left panel) with eS25 and eL13a, ribosomal proteins of the 40S and 60S ribosomal subunits, respectively. Although this result suggested that RACK1-FLAG was incorporated into polysomes, we could not exclude that it sedimented in heavy sucrose fractions because it formed aggregates. To further validate that RACK1-FLAG indeed was incorporated into polysomes, we treated cell lysate with puromycin. Puromycin is a tRNA analog, which stalls translation elongation and releases the growing peptide chain. When cell lysate treated with puromycin is heated to 37°C, the two ribosomal subunits are separated, and the mRNA is released (50). Puromycin treatment alters the sedimentation pattern for

ribosomal proteins, which now sediment in lighter sucrose fractions where the ribosomal protein subunits are found. Following puromycin treatment, RACK1-FLAG now sedimented in the lighter sucrose gradient fractions 3 and 4 (figure 1C, right panel), where it again co-sediments with eS25. Taken together, these results indicate that RACK1-FLAG is incorporated into translating ribosomes and likely fully functional.

RACK1 mediates translation of viral IRESs

Loss of RACK1 has been previously shown to inhibit translation of the HCV and CrPV 5′ IRES (47) raising the possibility that RACK1 generally facilitates viral IRES-mediated translation. To test this hypothesis, we used dicistronic luciferase reporters, in which translation of the *Renilla* luciferase uses canonical cap-dependent translation initiation, while translation of the Firefly luciferase is mediated by a viral IRES (figure 2A). We tested the importance of RACK1 for translation of four viral IRESs, specifically PV, EMCV, HCV and CrPV intergenic IRESs. These IRESs represent four major types of viral IRESs and use different mechanisms for translation initiation (4). None of these viral IRESs use the cap-binding function of eIF4E, although a recent study showed that eIF4E stimulates the helicase activity of eIF4A on the PV IRES independent of its cap-binding function (52). In contrast to PV, neither the EMCV nor the HCV IRES use a scanning mechanism but instead directly recruit the ribosome to the start codon (53). While the EMCV IRES requires all canonical translation initiation factors except for eIF4E, translation initiation of the HCV IRES uses a more limited set of

translation initiation factors. In agreement with previous observations, loss of RACK1 did not alter translation of the CrPV intergenic (IGR) IRES, but inhibited translation of the HCV IRES (figures 2B and 2C, and (47)). In addition, we observed that RACK1 also facilitated translation of the EMCV and PV IRESs (figures 2B and 2C). Expression of RACK1-FLAG in RACK1 knockout cells partially rescued the defect in IRES-mediated translation (figure 2C). The observed rescue approximately corresponded to the expression level of RACK1-FLAG (figures 2C and 1A). Taken together, these data support the need for RACK1 to facilitate translation of HCV, EMCV and PV IRESs, but not CrPV IGR IRES.

PV plaque diameters are decreased in cells lacking RACK1

To test if the reduction of PV IRES-mediated translation impacts the virus during infection, we performed PV plaque assays in wildtype, RACK1 KO #1, and RACK1-FLAG add-back cells and measured both PV plaque diameter and plaque numbers. Following infection with the Mahoney strain of PV, we observed a significant decrease in the PV plaque size in cells lacking RACK1 as compared to wildtype and RACK1-FLAG add-back cells (figure 3A). In contrast, the number of PV plaques was not significantly altered in any of the cell lines (figure 3B). Together, these data indicate that infectious particles are similarly efficient at establishing an infection independent of cellular RACK1 levels, however, the infectious cycle and virus spread may be impaired.

Loss of RACK1 impairs PV translation during the entire virus life cycle

Upon PV infection, the PV genome must be translated to give rise to the viral proteins, which include the viral proteases 2A and 3C. When levels of 2A and 3C are sufficiently high, these viral proteases cleave translation factors eIF4G and PABP, which shuts off translation in the host cell. Our observation that PV plaques are reduced in cells lacking RACK1 made us wonder whether loss of RACK1 prolonged the viral life cycle and delayed host-cell translation shut-off. To test whether translational shut-off was delayed in RACK1 KO cells, we performed ^{35}S pulse-labeling experiments in mock-infected and PV-infected cells at a multiplicity of infection (MOI) of 1. When newly synthesized proteins were metabolically labeled 3 hours 5 minutes post infection and lysates revolved by SDS-PAGE we observed that wildtype and RACK1-FLAG add-back cells started to show the characteristic PV banding pattern observed in the positive control of cells infected at MOI = 10 and harvested at the same time (figure 4A) (16). In contrast, the protein pattern in the RACK1 KO cell lines was similar to the pattern in the mock-infected cells, in that cellular proteins were metabolically labeled, and viral proteins are absent. These data indicate that the time until PV-induced translational shut-off of the host cell was indeed delayed (figure 4A). We next asked if PV translation also remained at lower levels in RACK1 KO cells post translational shut-off. To address this question, we monitored translation of a PV-Luciferase replicon (PV-Luc) during the initial phase of translation and translation during viral replication. Instead of the viral structural proteins, the PV-Luc replicon encodes a luciferase open reading frame fused to the PV non-structural proteins.

212 Early during infection, luciferase measurements reveal initial translation of the
213 replicon. Once negative strand synthesis has occurred, the PV genome will start
214 replicating, which will result in greater translation of the replicon and largely
215 increased luciferase production. We transfected *in vitro* transcribed PV-Luc RNA
216 into wildtype, RACK1 KO #1 and RACK1-FLAG cells, harvested protein lysates
217 3, 5, 7, and 9 hours post transfection and measured luciferase levels by
218 luminescence. As expected, we observed robust luciferase production in wildtype
219 cells, while levels of luciferase in RACK1 KO #1 remained more than 10-fold
220 lower (figure 4B, top panel). Consistent with our previous results, RACK1-FLAG
221 expression in the KO cell line partially rescued luciferase expression. To help
222 distinguish viral translation and replication stages, we immediately treated cells
223 with guanidine hydrochloride, a drug that inhibits viral replication (54). Thus, the
224 measured amount of luciferase produced in these experiments only represents
225 protein production prior to viral replication. Although luciferase levels in RACK1
226 KO#1 and RACK1-FLAG cells were comparable at 3 hours post transfection,
227 luciferase levels in the RACK1-FLAG cell line increased over time, reaching
228 levels comparable to luciferase levels in wildtype cells, while cells lacking RACK1
229 KO#1 failed to accumulate significant levels of luciferase (figure 4B, middle
230 panel). When cells were treated with the translation inhibitor cycloheximide
231 immediately after PV-Luc reporter transfection, luciferase levels measured in all
232 cells were at background levels (figure 4B, lower panel), indicating that
233 translation of the viral genome had been completely blocked.
234

Taken together, this data indicates that RACK1 not only mediates translation of the HCV IRES but is also critical for efficient translation of the EMCV and PV IRESs using dicistronic luciferase assays. Cells lacking RACK1 also show a reduced PV plaque size, likely due to inefficient PV translation prior to as well as post host cell translational shut-off, which further extends the PV life cycle.

Discussion

The ribosomal protein RACK1 interacts with numerous cellular proteins and has been thought to function as a scaffolding protein that connects cellular signaling pathways with the ribosome and the translation machinery (55). In addition, it has been previously shown that RACK1 is important for translation of the HCV IRES (47). Although HCV, PV and EMCV all use IRESs for translation initiation, the PV and EMCV IRESs rely on more translation factors than the HCV IRES. These translation factors could compensate for the function of RACK1, which prompted us to test whether RACK1 is also needed for translation of other viral IRESs. We thus employed RACK1 knockout cells generated by CRISPR-Cas9 mediated genome editing (45) and transduced them with lentiviruses to express RACK1-FLAG, which was incorporated into translating ribosomes (figure 1). In contrast to others who have reported that RACK1 depletion reduces cap-dependent translation (30, 56), we do not observe major changes in cap-dependent translation in RACK1 KO cells ((45), figure 4A and unpublished data). It is possible that the contrasting observations are due to cell line specific differences. While HAP1 cells are derived from the chronic myelogenous leukemia (CML) cell

line KBM-7, all studies that found that RACK1 influenced cap-dependent and -independent translation were performed in HEK293, HEK293T, and HeLa cells (30, 31, 56). Since RACK1 stimulates global translation in a PKCβII-dependent manner (30, 43), potentially higher PKCβII expression levels found in HEK293 and HeLa cells or other cell line-specific differences might explain the opposing effect on translation ((57), https://www.proteinatlas.org/ENSG00000166501-PRKCB/cell).

To test the involvement of RACK1 in IRES-mediated translation beyond CrPV and HCV IRESs, we used dicistronic luciferase constructs (figure 2A) containing the EMCV and PV IRESs, two other well-characterized viral IRESs. We found that RACK1 not only facilitates translation of the HCV IRES, but also of the EMCV and PV IRESs (figure 2). In agreement with previous work by Majzoub et al., translation of the CrPV IGR IRES occurred in a RACK-independent manner (47). To examine if RACK1 also plays a critical role during PV infection, we next infected wildtype, RACK1 KO and RACK1-FLAG expressing cells with the Mahoney strain of PV and performed plaque assays. While loss of RACK1 caused significantly smaller PV plaques (figure 3A), almost all infectious particles are able to start a successful infection (figure 3B). This finding indicates that RACK1 is partially dispensable for PV IRES-mediated translation, but also suggests that RACK1 specifically influences the translation efficiency of the PV IRES-containing RNA. Several groups have found RACK1 to regulate autophagy by directly interacting with Atg5 (58) and by enhancing Atg14L-Beclin 1-Vps34-Vps15 complex formation (59). However, neither Atg5 nor Beclin 1 impact PV

proliferation (60) making it unlikely that the observed phenotype is due to changes in the autophagy pathway.

Using metabolic labeling and translation of a PV-Luc reporter we further showed that PV translation is attenuated in cells lacking RACK1 (figure 4) both pre and post translational shut-off (figure 4B). Decreased PV translation early during the virus life cycle lengthens the time until critical quantities of poliovirus proteases 2A and 3C are produced. These two proteases cleave translation factors eIF4G and PABP, respectively, cause host cell translation shut-off and enable viral replication (11, 14, 61). In cells lacking RACK1, translational shut-off of the host cell takes longer compared to RACK1-expressing cells (figure 4A). Further, RACK1 is not only critical prior to translational shut-off, but our PV-Luc reporter assay also showed that cells lacking RACK1 do not efficiently replicate the PV genome, while cells expressing RACK1 start replication 3h post transfection (figure 4B, top panel). Although RACK1 is not essential for PV translation, it enhances the translation efficiency of PV and other viruses, indicating RACK1 acts as a pro-viral host protein.

Interestingly, our findings are reminiscent of ribosomal protein eS25, previously shown to mediate both viral and cellular IRES-mediated translation (19, 20). Both eS25 and RACK1 have a greater impact on HCV IRES translation, reducing IRES activity by about 75%, while translation of the PV IRES is less sensitive to eS25 and RACK1 levels. Curiously, the EMCV IRES appears to depend more on RACK1 than eS25, since loss of RACK1 causes a 60% decrease in IRES

activity, while loss of eS25 only decreases EMCV IRES activity by 40%. Similarly, though, shRNA-mediated depletion of eS25 resulted in a 2-fold decrease in PV viral titers (20), which indicates that loss of eS25 might also lengthen the viral life cycle prior and post translational shut-off, however, no PV plaque size of a direct virus plaque assay was reported. In contrast to RACK1, eS25 reduction was found to inhibit all viral IRESs, including the CrPV IGR IRES (19). Both RACK1 and eS25 are ribosomal proteins that are usurped by viruses to enhance viral translation.

Our findings may be explained by three potential models for how RACK1 acts on PV translation. First, RACK1 could directly enhance the affinity of the ribosome for the PV IRES, for example by stabilizing IRES docking. Indeed, Landry et al. showed that the CrPV IRES is unable to bind to 40S ribosomal subunits lacking eS25 (19). Since the 40S ribosomal subunit is not directly recruited by the PV IRES but involves a scanning mechanism, *in vitro* ribosome affinity can only be measured in the presence of purified translation initiation factors, which is quite challenging. However, 40S ribosomal subunits lacking RACK1 directly bind the HCV IRES with an affinity similar to wildtype 40S ribosomal subunits (48). Further, ribosomes lacking RACK1 are also able to form 80S ribosomes at high concentrations of magnesium (48) indicating that RACK1 is neither involved in 40S nor 80S:HCV IRES complex formation. Although we cannot exclude a direct contribution of RACK1 to 40S binding or 80S complex formation with the EMCV

and PV IRESs, we believe that the evidence for the HCV IRES suggests that RACK1 might employ a mechanism distinct from eS25.

Second, RACK1 might directly or indirectly affect the structure of the ribosome:PV IRES complex, for example by stabilizing a translation-favorable IRES conformation. Such structural rearrangement has been observed for the HCV IRES (24) where domain 2 of the HCV IRES, which interacts with eS25, undergoes a ~55 Å movement. This movement switches the 40S ribosomal subunit from an open conformation for mRNA loading to a closed conformation with the initiator tRNA tightly bound to the P-site (24). Although domain II of the HCV IRES does not contribute to the binding affinity of the HCV IRES to the 40S ribosomal subunit (21, 62, 63), eS25 has been shown to have a critical function for HCV IRES translation (19, 23). The increased size of the PV IRES, which is almost double the size of the HCV IRES, and the complex translation initiation pathway of the PV IRES involving ribosome scanning and several more translation initiation factors has prevented the acquisition of a cryo-EM structure to test these models. Thus, in cell structure probing techniques such as selective 2′-hydroxyl acylation analyzed by primer extension (SHAPE) coupled with the replication inhibitor guanidine hydrochloride, may be required to provide valuable insights into the PV-IRES ribosome structure in the future (64).

Third, RACK1 is not near the HCV IRES binding interface as revealed by the cryo-EM structure of the HCV IRES:40S complex, further indicating that RACK1 unlikely affects IRES binding. In contrast to the CrPV IGR IRES, both the 5′ CrPV and HCV IRESs require eIF3, which has an extensive binding surface on the 40S

ribosomal subunit. Translation initiation factor eIF3 is composed of 13 protein subunits and binds to a large surface of the 40S ribosomal subunit (65, 66). While several eIF3 subunits are essential for its function, other factors such as eIF3H and eIF3J are dispensable (47, 67). Of these dispensable functions, loss of eIF3J mimics the RACK1 loss-of-function phenotype on HCV and CrPV 5′ IRES translation (47), possibly by altering the conformation of the mRNA entry channel (48). Again, the lack of a cryo-EM structure of the large PV IRES bound to the 40S ribosomal subunits prevents us from using structural data to gain insights into the mechanism of RACK1 on PV translation. Instead, biological approaches such as crosslinking-immunoprecipitation (CLIP) on PV-infected cells will have to be used to identify potential interactions between RACK1 and the PV IRES (68).

Although it is unclear how RACK1 facilitates PV translation and if the way RACK1 is used by PV is identical to HCV translation, the similarities to eS25 roles in IRES-mediated translation are striking. While the two ribosomal proteins appear to use distinct mechanisms, both might alter the conformation of the mRNA entry channel and/or the transitioning between the open and closed 40S conformation (24, 47). These findings further raise the question which cellular RNAs are translationally regulated by RACK1 and eS25 and whether the mRNA targets are distinctly different. The observations that neither RACK1 nor eS25 are largely involved in canonical cap-dependent translation (19, 45) suggests that the specific cellular mRNAs relying on these proteins might be translationally highly

372 regulated. Hertz et al. found that cellular IRES-containing mRNAs are less
373 efficiently translated in eS25-depleted cells (20), indicating a role of eS25 in cap-
374 independent translation. However, given the indirect interaction of RACK1 with
375 the HCV IRES via eIF3, further studies will be needed to determine if RACK1
376 also facilitates cap-independent translation or if it acts a translational enhancer of
377 specific mRNAs (69).
378
379 Ribosomal protein RACK1 not only enhances translation of HCV and the CrPV 5'
380 IRES, it also enhances translation of other viral IRES-containing RNAs such as
381 EMCV and PV. PV-infected cells lacking RACK1 inefficiently translate the viral
382 RNA, which lengthens the virus life cycle. These results suggest that targeting
383 RACK1 could be used as an antiviral strategy, but more research into the cellular
384 mRNAs that rely on RACK1 for translation is needed.
385

386 ## Materials and Methods

387 ### Cell culture

388 HAP1 cells purchased from Horizon USA (C859), HAP1-derived RACK1
389 knockout cell lines #1 and #2 (45), and RACK1-FLAG addback cell lines were
390 cultured in Iscove's modified Dulbecco's medium (IMDM; Corning) supplemented
391 with 5% fetal bovine serum and 2 mM L-glutamine. HEK293FT cells (Thermo
392 Scientific) grown in DMEM (Gibco) supplemented with 5% fetal bovine serum
393 and 2 mM L-glutamine were used to generate lentivirus particles for cellular

394 transductions. Cultures were confirmed negative for mycoplasma using DAPI
395 staining.
396
397 **Viral-Transduction of RACK1 Add-Back Cell Line**
398 RACK1 cDNA was cloned with primers Forward
399 5′ATGACTGAGCAGATGACCCTTCG3' and Reverse
400 5′CTAGCGTGTGCCAARGGTCACC3' from HeLa cells. RACK1-FLAG
401 expression construct was PCR-amplified from cDNA with Phusion polymerase
402 (NEB) with primers CACCATGACTGAGCAGATGACCCTTCGTG
403 TTATCACTTATCGTCGTCATCCTTGTAATCGCGTGTGCCAATGGTCACCTGC
404 CAC and cloned into pENTR D-TOPO vector. Using Gateway LR Clonase II
405 (Invitrogen) RACK1-FLAG was cloned into pLenti CMV Puro DEST (w118-1)
406 (Addgene plasmid #17452) following the manufacturer's protocol. RACK1-FLAG
407 was expressed in RACK1 KO#1 cell line following lentiviral transduction. For
408 lentivirus transduction, HEK293 FT cells (ThermoFisher) were co-transfected
409 with plasmids pCMV-dR8.2 dvpr (gag-pol; Addgene #8455), pCMV-VSV-G
410 (envelope; Addgene #8454), pAdVantage (Promega E1711) and pLenti RACK1-
411 FLAG using Fugene HD (Promega). The lentivirus-containing media was filtered
412 through a 0.45 µm PES filter. Following addition of 8 µg/ml protamine sulfate the
413 supernatant was used to transduce RACK1 KO #1 cells. Cultures transduced
414 overnight were selected with 1 µg/ml puromycin (InvivoGen) to generate a pool of
415 stably expressing RACK1-FLAG cells. Selection was complete when
416 untransduced RACK1 KO #1 cells had died.

417

418 **Polysome Profile Analysis**

419 Polysome profile analyses were performed on a 10 cm dish of approximately
420 80%-90% confluency in 10-50% sucrose gradients containing either in 500 mM
421 KCl, 15 mM Tris-HCl pH 7.5, 15 mM $MgCl_2$, 1 mg/ml heparin (Sigma) and 100
422 µg/ml cycloheximide (Sigma) or 500 mM KCl; 15 mM Tris-HCl, pH 7.5; 2 mM
423 $MgCl_2$; 1 mg/ml heparin (Sigma), 2 mM puromycin as previously described by
424 Fuchs et al. (70).

425

426 **Immunoblotting**

427 Total protein lysate was harvested in RIPA buffer (70), and proteins
428 separated by 12% SDS-PAGE were transferred to a nitrocellulose membrane
429 (GE Healthcare) for 70 Vh at 4˚C. Following transfer, membranes were blocked
430 in 1% milk in PBS for 30 minutes at room temperature, washed three times in
431 phosphate buffered saline with 0.1% (w/v) Tween 20 (PBS/T) for 10 minutes
432 each and placed in primary antibody overnight at 4˚C. Primary antibodies used
433 were rabbit RACK1 (1:2000 dilution, Cell Signaling #4716S), FLAG-HRP (1:1000,
434 Sigma-Aldrich, #F2555), L13a (1:1000, Cell Signaling #2765S), actin (1:1000,
435 Sigma-Aldrich #A2066) and RPS25 (1:1000, abcam, #ab102940). Following
436 overnight incubation, membranes were washed three times in PBS/T for 10
437 minutes each. For visualization of the HRP-conjugated FLAG antibody,
438 membranes were directly imaged on a BioRad ChemiDoc XRS+. For all other
439 antibodies, membranes were incubated in a 1:10,000 dilution of goat anti-rabbit

secondary (Jackson) in 5% milk and PBS/T. Membranes were washed a final 3 times in PBS/T for 10 minutes each prior to being imaged on the BioRad ChemiDoc XRS+.

Dual-Luciferase Assays

Bicistronic DNA constructs with *Renilla* and Firefly luciferase sequences flanked a viral IRES sequence. Viral IRESs evaluated were hepatitis C virus (HCV), cricket paralysis virus (CrPV), poliovirus (PV), and encephalomyocarditis virus (EMCV) (all gifts from Peter Sarnow, Stanford, USA). Approximately 20,000 cells of each cell line were seeded in the wells of a 96-well plate. For each construct, 100 ng DNA was transfected using lipofectamine 3000 reagent in accordance with the manufacturer's instructions (ThermoFisher). After 24 hours, cells were lysed in 50 µl 1X passive lysis buffer (Promega) and 20 µl sample was read for 10s in a Glomax 20/20 luminometer (Promega) using the dual-luciferase assay reagent (Promega #E1910). Averages of the Firefly over *Renilla* ratio of at least three independent replicates and the standard error of the mean were calculated and plotted after normalization to wildtype cells (100%, dotted line). Following normalization to wildtype cells, statistical analysis was performed by Student's t-test (two-tailed, unequal variance) and p-values are indicated in figure.

Poliovirus Plaque Assays

462 Approximately 2 million cells were seeded into 60 mm dishes the day prior
463 to infection. Cells were washed in PBS+ (PBS supplemented with 10 mg/ml
464 $MgCl_2$ and 10 mg/ml $CaCl_2$) and 100 µl diluted poliovirus was used to infect cells
465 for 30 minutes at 37˚C, 5% CO_2. Cells were covered with 1% bactoagar-media
466 mixture (DMEM supplemented with 5% fetal bovine serum and 2 mM L-
467 glutamine). After 40 hours at 37˚C, 5% CO_2, the agar layer and cells were fixed
468 and stained for 30 minutes at RT with a crystal violet solution containing 1%
469 formaldehyde, crystal violet and 20% ethanol. PV plaque sizes were determined
470 by measuring the plaque diameter in pixels using ImageJ (NIH). Poliovirus
471 plaques were counted, and average and standard error of the mean of three
472 independent replicates were plotted. P-values were determined via Student's t-
473 test (two-tailed, unequal variance).
474
475
476 **^{35}S metabolic labeling**
477 Wildtype, RACK1 KO #1 and #2, and RACK1-FLAG expressing cells were either
478 mock-infected or infected with PV Mahoney at MOI = 1 (MOI = 10 for positive
479 control) for 30 minutes at 37˚C, 5% CO_2. Cells were incubated for 3 hours and 5
480 minutes at 37˚C, 5% CO_2, then media was exchanged for DMEM lacking
481 cysteine and methionine (Corning®). After starvation for 30 min, cells were
482 metabolically labeled for 10 min with 10 µCi EasyTag™ EXPRESS^{35}S Protein
483 Labeling Mix (Perkin Elmer). Total cell lysate was harvested in RIPA buffer (70)

484 and separated by 10% SDS-PAGE. The dried gel was exposed to a phosphor-
485 screen (GE) and scanned using a Typhoon scanner (GE).
486
487 **Poliovirus Reporter Translation Assay**
488 The luciferase-expressing, poliovirus-derived replicon plasmid prib(+)Luc-Wt was
489 linearized with Mlu I (71) and *in vitro* transcribed with HiScribe T7 Quick High
490 Yield RNA Synthesis Kit (NEB) as previously described (52). Wildtype, RACK1
491 KO #1 and #2, and RACK1-FLAG expressing cells were trypsinized,
492 resuspended and gently pelleted. For each transfection reaction, approximately
493 $3x10^6$ cells were resuspended in 500 µl of media and reverse transfected in
494 suspension with Lipofectamine 3000 following the manufacturer's transfection
495 protocol for a 6-well plate. Immediately after transfection, three aliquots of 250 µl
496 of transfected cells were mixed with 500 µl of IMDM media each. To inhibit
497 translation, one aliquot of transfected cells was treated with 25 µg/ml
498 cyloheximide (Sigma). In a second aliquot, PV replicon replication was inhibited
499 with 2 mM guanidine hydrochloride. Aliquots of 150 µl were removed 3, 5, 7 and
500 9 h post transfection and luminescence was measured with luciferase assay
501 reagent (Promega) using a Glomax luminometer (Promega).
502
503 **Acknowledgements**
504 We thank Peter Sarnow (Stanford) his kind gift of viral IRES plasmids. The
505 prib(+)Luc-Wt plasmid was a kind gift from Raul Andino (UCSF). We further
506 thank Sangeetha Selvam and Cara Pager for discussions and for critically

reading the manuscript. This work was supported by start-up funds from the University at Albany, State University of New York, and the University at Albany Faculty Research Awards Program (FRAP) (to GF).

Conflict of interest: The authors declare that they have no conflict of interest with the contents of this article. The content is solely the responsibility of the authors.

Author contributions: EL, CMM, and GF designed the study and wrote the paper. CMM performed RACK1 immunoblot and quantification, and 35S pulse-labeling experiment EL performed polysome and PV plaque assay experiments. EL and NP performed the dual luciferase assays, and EL and GF performed the cell-based PV-Luc replicon experiments. AJ cloned the RACK1-FLAG construct for lentivirus transduction, and ETM performed statistical analysis. All authors analyzed the data and approved the final version of the paper.

References

1. Wek RC, Jiang H-Y, Anthony TG. 2006. Coping with stress: eIF2 kinases and translational control. Biochem Soc Trans 34:7–11.
2. Pakos-Zebrucka K, Koryga I, Mnich K, Ljujic M, Samali A, Gorman AM. 2016. The integrated stress response. EMBO Rep 17:1374–1395.
3. Wek RC. 2018. Role of eIF2α Kinases in Translational Control and Adaptation to Cellular Stress. Cold Spring Harb Perspect Biol 10:a032870.
4. Clarke PA, Schwemmle M, Schickinger J, Hilse K, Clemens MJ. 1991. Binding of Epstein-Barr virus small RNA EBER-1 to the double-stranded RNA-activated protein kinase DAI. Nucleic Acids Res 19:243–8.
5. Sharp T V, Schwemmle M, Jeffrey I, Laing K, Mellor H, Proud CG, Hilse K, Clemens MJ. 1993. Comparative analysis of the regulation of the interferon-inducible protein kinase PKR by Epstein-Barr virus RNAs EBER-1 and EBER-2 and adenovirus VAI RNA. Nucleic Acids Res 21:4483–90.
6. Ghadge GD, Swaminathan S, Katze MG, Thimmapaya B. 1991. Binding of the adenovirus VAI RNA to the interferon-induced 68-kDa protein kinase correlates with function. Proc Natl Acad Sci U S A 88:7140–4.
7. Langland JO, Pettiford S, Jiang B, Jacobs BL. 1994. Products of the porcine group C rotavirus NSP3 gene bind specifically to double-stranded RNA and inhibit activation of the interferon-induced protein kinase PKR. J Virol 68:3821–9.
8. Black TL, Safer B, Hovanessian A, Katze MG. 1989. The cellular 68,000-Mr protein kinase is highly autophosphorylated and activated yet

545 significantly degraded during poliovirus infection: implications for
546 translational regulation. J Virol 63:2244–51.
547 9. Hebner CM, Wilson R, Rader J, Bidder M, Laimins LA. 2006. Human
548 papillomaviruses target the double-stranded RNA protein kinase pathway.
549 J Gen Virol 87:3183–3193.
550 10. Ventoso I, MacMillan SE, Hershey JW, Carrasco L. 1998. Poliovirus 2A
551 proteinase cleaves directly the eIF-4G subunit of eIF-4F complex. FEBS
552 Lett 435:79–83.
553 11. Svitkin Y V, Gradi A, Imataka H, Morino S, Sonenberg N. 1999. Eukaryotic
554 initiation factor 4GII (eIF4GII), but not eIF4GI, cleavage correlates with
555 inhibition of host cell protein synthesis after human rhinovirus infection. J
556 Virol 73:3467–72.
557 12. Kuyumcu-Martinez NM, Joachims M, Lloyd RE. 2002. Efficient cleavage of
558 ribosome-associated poly(A)-binding protein by enterovirus 3C protease. J
559 Virol 76:2062–74.
560 13. Kuyumcu-Martinez NM, Van Eden ME, Younan P, Lloyd RE. 2004.
561 Cleavage of poly(A)-binding protein by poliovirus 3C protease inhibits host
562 cell translation: a novel mechanism for host translation shutoff. Mol Cell
563 Biol 24:1779–90.
564 14. Bonderoff JM, Larey JL, Lloyd RE. 2008. Cleavage of poly(A)-binding
565 protein by poliovirus 3C proteinase inhibits viral internal ribosome entry
566 site-mediated translation. J Virol 82:9389–99.
567 15. de Breyne S, Bonderoff JM, Chumakov KM, Lloyd RE, Hellen CUT. 2008.

568 Cleavage of eukaryotic initiation factor eIF5B by enterovirus 3C proteases.
569 Virology 378:118–122.
570 16. White JP, Reineke LC, Lloyd RE. 2011. Poliovirus Switches to an eIF2-
571 Independent Mode of Translation during Infection. J Virol 85:8884–8893.
572 17. Pelletier J, Sonenberg N. 1988. Internal initiation of translation of
573 eukaryotic mRNA directed by a sequence derived from poliovirus RNA.
574 Nature 334:320–325.
575 18. Lee AS-Y, Burdeinick-Kerr R, Whelan SPJ. 2013. A ribosome-specialized
576 translation initiation pathway is required for cap-dependent translation of
577 vesicular stomatitis virus mRNAs. Proc Natl Acad Sci U S A 110:324–9.
578 19. Landry DM, Hertz MI, Thompson SR. 2009. RPS25 is essential for
579 translation initiation by the Dicistroviridae and hepatitis C viral IRESs.
580 Genes Dev2009/12/03. 23:2753–2764.
581 20. Hertz MI, Landry DM, Willis AE, Luo G, Thompson SR. 2013. Ribosomal
582 protein s25 dependency reveals a common mechanism for diverse internal
583 ribosome entry sites and ribosome shunting. Mol Cell Biol 33:1016–26.
584 21. Spahn CM, Kieft JS, Grassucci RA, Penczek PA, Zhou K, Doudna JA,
585 Frank J. 2001. Hepatitis C virus IRES RNA-induced changes in the
586 conformation of the 40s ribosomal subunit. Science (80-) 291:1959–1962.
587 22. Nishiyama T, Yamamoto H, Uchiumi T, Nakashima N. 2007. Eukaryotic
588 ribosomal protein RPS25 interacts with the conserved loop region in a
589 dicistroviral intergenic internal ribosome entry site. Nucleic Acids Res
590 35:1514–1521.

591 23. Muhs M, Yamamoto H, Ismer J, Takaku H, Nashimoto M, Uchiumi T,
592 Nakashima N, Mielke T, Hildebrand PW, Nierhaus KH, Spahn CM. 2011.
593 Structural basis for the binding of IRES RNAs to the head of the ribosomal
594 40S subunit. Nucleic Acids Res2011/03/08.
595 24. Yamamoto H, Collier M, Loerke J, Ismer J, Schmidt A, Hilal T, Sprink T,
596 Yamamoto K, Mielke T, Bürger J, Shaikh TR, Dabrowski M, Hildebrand
597 PW, Scheerer P, Spahn CMT. 2015. Molecular architecture of the
598 ribosome-bound Hepatitis C Virus internal ribosomal entry site RNA.
599 EMBO J 34:3042–58.
600 25. Gerbasi VR, Weaver CM, Hill S, Friedman DB, Link AJ. 2004. Yeast Asc1p
601 and Mammalian RACK1 Are Functionally Orthologous Core 40S
602 Ribosomal Proteins That Repress Gene Expression. Mol Cell Biol
603 24:8276–8287.
604 26. Sengupta J, Nilsson J, Gursky R, Spahn CMT, Nissen P, Frank J. 2004.
605 Identification of the versatile scaffold protein RACK1 on the eukaryotic
606 ribosome by cryo-EM. Nat Struct Mol Biol 11:957–962.
607 27. Coyle SM, Gilbert W V., Doudna JA. 2009. Direct Link between RACK1
608 Function and Localization at the Ribosome In Vivo. Mol Cell Biol 29:1626–
609 1634.
610 28. Anger AM, Armache J-P, Berninghausen O, Habeck M, Subklewe M,
611 Wilson DN, Beckmann R. 2013. Structures of the human and Drosophila
612 80S ribosome. Nature 497:80–5.
613 29. Chang BY, Chiang M, Cartwright CA. 2001. The interaction of Src and

RACK1 is enhanced by activation of protein kinase C and tyrosine phosphorylation of RACK1. J Biol Chem 276:20346–56.

30. Dobrikov MI, Dobrikova EY, Gromeier M. 2018. Ribosomal RACK1:Protein Kinase C βII Phosphorylates Eukaryotic Initiation Factor 4G1 at S1093 To Modulate Cap-Dependent and -Independent Translation Initiation. Mol Cell Biol 38.

31. Dobrikov MI, Dobrikova EY, Gromeier M. 2018. Ribosomal RACK1:Protein Kinase C βII Modulates Intramolecular Interactions between Unstructured Regions of Eukaryotic Initiation Factor 4G (eIF4G) That Control eIF4E and eIF3 Binding. Mol Cell Biol 38.

32. Jannot G, Bajan S, Giguère NJ, Bouasker S, Banville IH, Piquet S, Hutvagner G, Simard MJ. 2011. The ribosomal protein RACK1 is required for microRNA function in both C. elegans and humans. EMBO Rep 12:581–586.

33. Ceci M, Gaviraghi C, Gorrini C, Sala LA, Offenhäuser N, Carlo Marchisio P, Biffo S. 2003. Release of eIF6 (p27BBP) from the 60S subunit allows 80S ribosome assembly. Nature 426:579–584.

34. Matsuda R, Ikeuchi K, Nomura S, Inada T. 2014. Protein quality control systems associated with no-go and nonstop mRNA surveillance in yeast. Genes to Cells 19:1–12.

35. Sundaramoorthy E, Leonard M, Mak R, Liao J, Fulzele A, Bennett EJ. 2017. ZNF598 and RACK1 Regulate Mammalian Ribosome-Associated Quality Control Function by Mediating Regulatory 40S Ribosomal

637 Ubiquitylation. Mol Cell 65:751-760.e4.
638 36. Kershner L, Welshhans K. 2017. RACK1 is necessary for the formation of
639 point contacts and regulates axon growth. Dev Neurobiol 77:1038–1056.
640 37. Wehner P, Shnitsar I, Urlaub H, Borchers A. 2011. RACK1 is a novel
641 interaction partner of PTK7 that is required for neural tube closure.
642 Development 138:1321–1327.
643 38. Volta V, Beugnet A, Gallo S, Magri L, Brina D, Pesce E, Calamita P,
644 Sanvito F, Biffo S. 2013. RACK1 depletion in a mouse model causes
645 lethality, pigmentation deficits and reduction in protein synthesis efficiency.
646 Cell Mol Life Sci 70:1439–1450.
647 39. Kadrmas JL, Smith MA, Pronovost SM, Beckerle MC. 2007.
648 Characterization of RACK1 function inDrosophila development. Dev Dyn
649 236:2207–2215.
650 40. Guo J, Chen J-G. 2008. RACK1 genes regulate plant development with
651 unequal genetic redundancy in Arabidopsis. BMC Plant Biol 8:108.
652 41. Guo J, Wang S, Valerius O, Hall H, Zeng Q, Li J-F, Weston DJ, Ellis BE,
653 Chen J-G. 2011. Involvement of Arabidopsis RACK1 in Protein Translation
654 and Its Regulation by Abscisic Acid. PLANT Physiol 155:370–383.
655 42. Thompson MK, Rojas-Duran MF, Gangaramani P, Gilbert W V. 2016. The
656 ribosomal protein Asc1/RACK1 is required for efficient translation of short
657 mRNAs. Elife 5.
658 43. Grosso S, Volta V, Sala LA, Vietri M, Marchisio PC, Ron D, Biffo S. 2008.
659 PKCβII modulates translation independently from mTOR and through

RACK1. Biochem J 415:77–85.

44. Romano N, Veronese M, Manfrini N, Zolla L, Ceci M. 2019. Ribosomal RACK1 promotes proliferation of neuroblastoma cells independently of global translation upregulation. Cell Signal 53:102–110.

45. Jha S, Rollins MG, Fuchs G, Procter DJ, Hall EA, Cozzolino K, Sarnow P, Savas JN, Walsh D. 2017. Trans-kingdom mimicry underlies ribosome customization by a poxvirus kinase. Nature 546.

46. Hertz MI, Thompson SR. 2011. Mechanism of translation initiation by Dicistroviridae IGR IRESs. Virology 411:355.

47. Majzoub K, Hafirassou ML, Meignin C, Goto A, Marzi S, Fedorova A, Verdier Y, Vinh J, Hoffmann JA, Martin F, Baumert TF, Schuster C, Imler J-L. 2014. RACK1 Controls IRES-Mediated Translation of Viruses. Cell 159:1086–1095.

48. Johnson AG, Lapointe CP, Wang J, Corsepius NC, Choi J, Fuchs G, Puglisi JD. 2019. RACK1 on and off the ribosome. bioRxiv 582635.

49. Carette JE, Raaben M, Wong AC, Herbert AS, Obernosterer G, Mulherkar N, Kuehne AI, Kranzusch PJ, Griffin AM, Ruthel G, Dal Cin P, Dye JM, Whelan SP, Chandran K, Brummelkamp TR. 2011. Ebola virus entry requires the cholesterol transporter Niemann-Pick C1. Nature 477:340–3.

50. Blobel G, Sabatini D. 1971. Dissociation of mammalian polyribosomes into subunits by puromycin. Proc Natl Acad Sci U S A 68:390–394.

51. Balvay L, Rifo RS, Ricci EP, Decimo D, Ohlmann T. 2009. Structural and functional diversity of viral IRESes. Biochim Biophys Acta - Gene Regul

683 Mech 1789:542–557.
684 52. Avanzino BC, Fuchs G, Fraser CS. 2017. Cellular cap-binding protein,
685 eIF4E, promotes picornavirus genome restructuring and translation. Proc
686 Natl Acad Sci U S A 114.
687 53. Kieft JS. 2008. Viral IRES RNA structures and ribosome interactions.
688 Trends Biochem Sci2008/05/13. 33:274–283.
689 54. Powers CD, Miller BA, Kurtz H, Ackermann WW. 1969. Specific effect of
690 guanidine in the programming of poliovirus inhibition of deoxyribonucleic
691 acid synthesis. J Virol 3:337–42.
692 55. Nielsen MH, Flygaard RK, Jenner LB. 2017. Structural analysis of
693 ribosomal RACK1 and its role in translational control. Cell Signal 35:272–
694 281.
695 56. Gallo S, Ricciardi S, Manfrini N, Pesce E, Oliveto S, Calamita P, Mancino
696 M, Maffioli E, Moro M, Crosti M, Berno V, Bombaci M, Tedeschi G, Biffo S.
697 2018. RACK1 Specifically Regulates Translation through Its Binding to
698 Ribosomes. Mol Cell Biol 38.
699 57. Uhlen M, Fagerberg L, Hallstrom BM, Lindskog C, Oksvold P, Mardinoglu
700 A, Sivertsson A, Kampf C, Sjostedt E, Asplund A, Olsson I, Edlund K,
701 Lundberg E, Navani S, Szigyarto CA-K, Odeberg J, Djureinovic D,
702 Takanen JO, Hober S, Alm T, Edqvist P-H, Berling H, Tegel H, Mulder J,
703 Rockberg J, Nilsson P, Schwenk JM, Hamsten M, von Feilitzen K,
704 Forsberg M, Persson L, Johansson F, Zwahlen M, von Heijne G, Nielsen J,
705 Ponten F. 2015. Tissue-based map of the human proteome. Science (80-)

347:1260419–1260419.

58. Erbil S, Oral O, Mitou G, Kig C, Durmaz-Timucin E, Guven-Maiorov E, Gulacti F, Gokce G, Dengjel J, Sezerman OU, Gozuacik D. 2016. RACK1 Is an Interaction Partner of ATG5 and a Novel Regulator of Autophagy. J Biol Chem 291:16753–65.

59. Zhao Y, Wang Q, Qiu G, Zhou S, Jing Z, Wang J, Wang W, Cao J, Han K, Cheng Q, Shen B, Chen Y, Zhang WJ, Ma Y, Zhang J. 2015. RACK1 Promotes Autophagy by Enhancing the Atg14L-Beclin 1-Vps34-Vps15 Complex Formation upon Phosphorylation by AMPK. Cell Rep 13:1407–1417.

60. Abernathy E, Mateo R, Majzoub K, van Buuren N, Bird SW, Carette JE, Kirkegaard K. 2019. Differential and convergent utilization of autophagy components by positive-strand RNA viruses. PLOS Biol 17:e2006926.

61. Gradi A, Svitkin Y V, Imataka H, Sonenberg N. 1998. Proteolysis of human eukaryotic translation initiation factor eIF4GII, but not eIF4GI, coincides with the shutoff of host protein synthesis after poliovirus infection. Proc Natl Acad Sci U S A 95:11089–94.

62. Kieft JS, Zhou K, Jubin R, Doudna JA. 2001. Mechanism of ribosome recruitment by hepatitis C IRES RNA. Rna 7:194–206.

63. Filbin ME, Vollmar BS, Shi D, Gonen T, Kieft JS. 2013. HCV IRES manipulates the ribosome to promote the switch from translation initiation to elongation. Nat Struct Mol Biol 20:150–8.

64. Burrill CP, Westesson O, Schulte MB, Strings VR, Segal M, Andino R.

729 2013. Global RNA structure analysis of poliovirus identifies a conserved
730 RNA structure involved in viral replication and infectivity. J Virol 87:11670–
731 83.
732 65. Hashem Y, des Georges A, Dhote V, Langlois R, Liao HY, Grassucci RA,
733 Pestova T V, Hellen CUT, Frank J. 2013. Hepatitis-C-virus-like internal
734 ribosome entry sites displace eIF3 to gain access to the 40S subunit.
735 Nature 503:539–43.
736 66. Yamamoto H, Unbehaun A, Loerke J, Behrmann E, Collier M, Bürger J,
737 Mielke T, Spahn CMT. 2014. Structure of the mammalian 80S initiation
738 complex with initiation factor 5B on HCV-IRES RNA. Nat Struct Mol Biol
739 21:721–7.
740 67. Johnson AG, Petrov AN, Fuchs G, Majzoub K, Grosely R, Choi J, Puglisi
741 JD. 2018. Fluorescently-tagged human eIF3 for single-molecule
742 spectroscopy. Nucleic Acids Res 46.
743 68. Gutiérrez-Escolano AL, Medina F, Racaniello VR, Del Angel RM. 1997.
744 Differences in the UV-Crosslinking Patterns of the Poliovirus 5′-
745 Untranslated Region with Cell Proteins from Poliovirus-Susceptible and -
746 Resistant Tissues. Virology 227:505–508.
747 69. Gilbert W V. 2010. Alternative Ways to Think about Cellular Internal
748 Ribosome Entry. J Biol Chem 285:29033–29038.
749 70. Fuchs G, Diges C, Kohlstaedt LA, Wehner KA, Sarnow P. 2011. Proteomic
750 Analysis of Ribosomes: Translational Control of mRNA Populations by
751 Glycogen Synthase GYS1. J Mol Biol 410:118–130.

752 71. Vogt DA, Andino R. 2010. An RNA element at the 5'-end of the poliovirus
753 genome functions as a general promoter for RNA synthesis. PLoS Pathog
754 6:e1000936.
755 72. Florez PM, Sessions OM, Wagner EJ, Gromeier M, Garcia-Blanco MA.
756 2005. The Polypyrimidine Tract Binding Protein Is Required for Efficient
757 Picornavirus Gene Expression and Propagation. J Virol 79:6172–6179.
758

Figure legends

Figure 1: RACK1-FLAG is incorporated into polysomes. (A) RACK1 levels can be partially restored in RACK1 KO cells by expression of RACK1-FLAG. RACK1 levels in the different cell lines were quantified on the immunoblot analysis of RACK1 and the loading control actin. (B) Polysome trace of HAP1 wildtype cells. Cell lysate was separated in 10-50% sucrose gradient and absorbance at 254 nm was measured. (C) Sucrose gradient analysis of FLAG-tagged RACK1 protein. In cells treated with the translation elongation inhibitor cycloheximide, RACK1-FLAG detected by immunoblotting using an anti-FLAG antibody co-sediments with polysomes (fractions 9-14). Upon treatment of cell lysate with the translation elongation puromycin, which separates actively translating ribosomes into the ribosomal subunits, RACK1-FLAG co-sediments with 40S ribosomal subunits in lighter sucrose gradient fractions (fractions 3-4). Immunoblot analysis for eS25 and uI13 are used as indicators for sedimentation of protein components of the small and large ribosomal subunits, respectively.

Figure 2: RACK1 facilitates translation of viral IRESs. (A). Schematic overview of dual luciferase construct used in assays. The *Renilla* luciferase open reading frame is translated via m7G cap-dependent translation, while the viral IRES located in the intergenic region between the two coding sequences mediates translation of the Firefly luciferase. (B) Translation efficiency of CrPV, HCV, PV and EMCV dual luciferase reporters in both RACK1 KO cells normalized to HAP1 cells (dotted line). Error bars represent the standard error of

782 the mean of at least three independent experiments. ** p-value < 0.01; *** p-
783 value < 0.001 (C) Translation of HCV, EMCV and PV IRESs correlates with
784 RACK1 levels, but translation of CrPV IGR IRES is RACK1 independent. Ratios
785 of Firefly/*Renilla* normalized to HAP1 ratios (dotted line). Error bars represent the
786 standard error of the mean of at least three independent experiments. * p-value <
787 0.05; ** p-value < 0.01; *** p-value < 0.001
788
789 **Figure 3: PV plaque size is reduced in cells lacking RACK1**
790 (A) Analysis of PV plaque assays. PV plaques in RACK1 KO #1 cells are smaller
791 compared to PV plaques in wildtype and RACK1-FLAG addback cells (left
792 panel). Cells were infected at identical MOI; 42h post infection, cells were stained
793 with crystal violet and poliovirus plaque diameters were measured. Error bars
794 represent the standard deviation within the population of three independent
795 experiments. The box indicates the data between the interquartile range (IQR)
796 between the 25th and 75th percentile, the median is indicated by the thick line
797 within the box. The thin vertical bars represent the minimum and maximum data
798 points (Q1-1.5*IQR, Q3+1.5*IQR). Outliers in the wildtype cells are indicated by
799 filled squares. (B) The number of visible poliovirus plaques does not differ
800 between wildtype, RACK1 KO #1 and RACK1-FLAG cell lines. Cells were
801 infected at identical MOI; 42h post infection, cells were stained with crystal violet
802 and poliovirus plaques were counted. Error bars represent the standard error of
803 the mean of at least three independent experiments.
804

Figure 4: RACK1 is required for efficient PV translation prior and post host cell translational shut-off. (A) ^{35}S metabolic pulse labeling of uninfected (mock) and PV-infected cells. Cells were mock-infected or infected with PV Mahoney at MOI = 1 (MOI = 10 for positive control) and ^{35}S pulse-labeled for 10 min at 3 hours and 5 min post infection. Total protein lysates were separated in 10% SDS-PAGE and visualized by exposure to a phosphor-screen. Poliovirus-specific protein products P1, 3CD, and 2C are indicated (72).

(B) Expression of a PV-Luc replicon is inefficient in cells lacking RACK1. HAP1, RACK1 KO #1, and RACK-1 FLAG cells were transfected with *in vitro* transcribed PV-Luc replicon RNA. An aliquot of cells was removed 3, 5, 7, and 9 hours post RNA transfection and Firefly luminescence was measured. Error bars represent the standard error of the mean of at least three independent experiments. Top panel: PV-Luc translation is decreased in cells lacking RACK1 during the replication phase. Middle panel: To limit the observation to the early translation phase, PV-Luc replication was inhibited with 2 mM guanidine hydrochloride immediately after RNA transfection. Bottom panel: Translation of all PV-Luc reporters is completely inhibited upon treatment with 25 µg/ml cycloheximide. Cells were treated with cycloheximide immediately after RNA transfection.

Figure 1

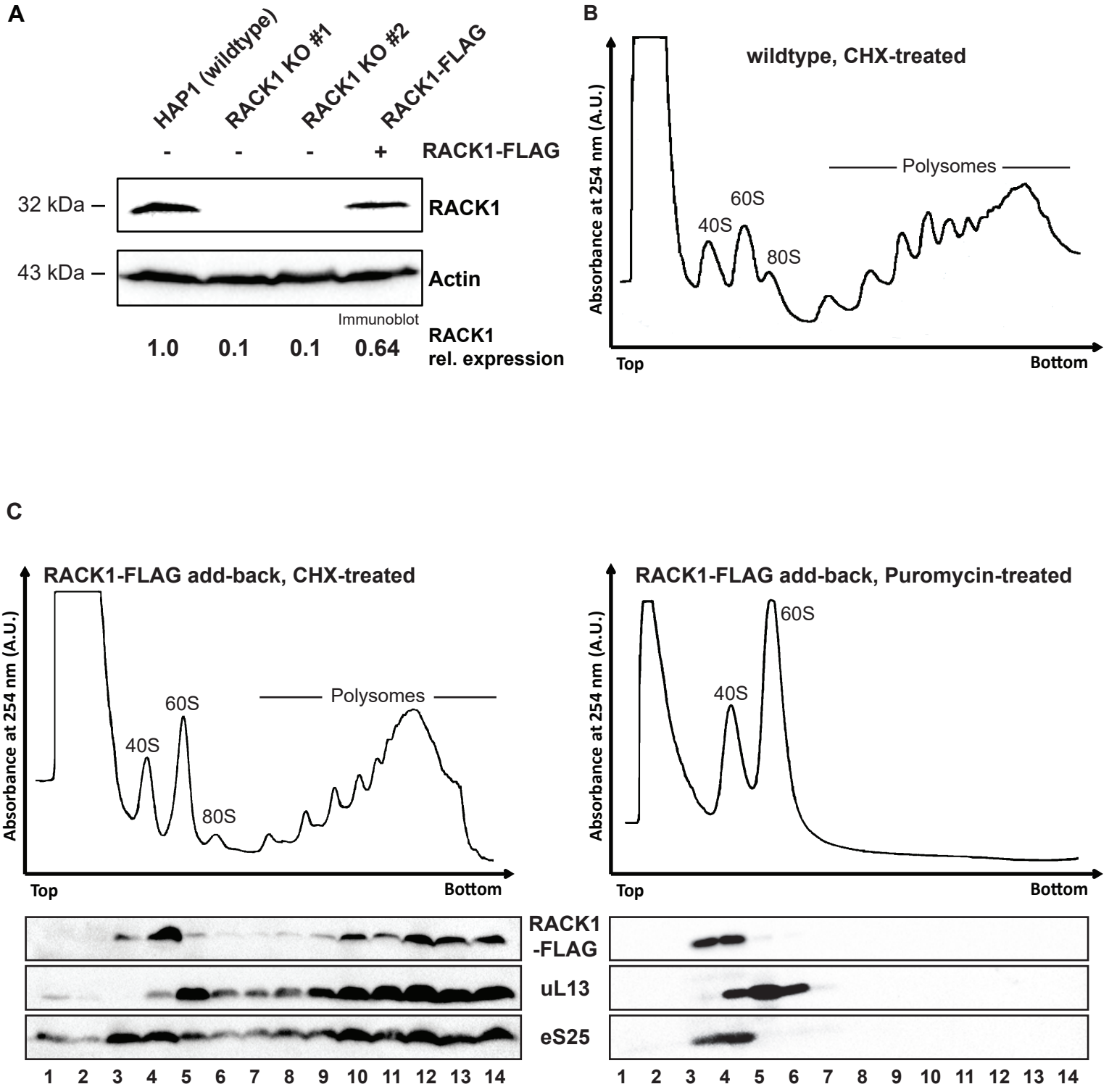

Figure 2

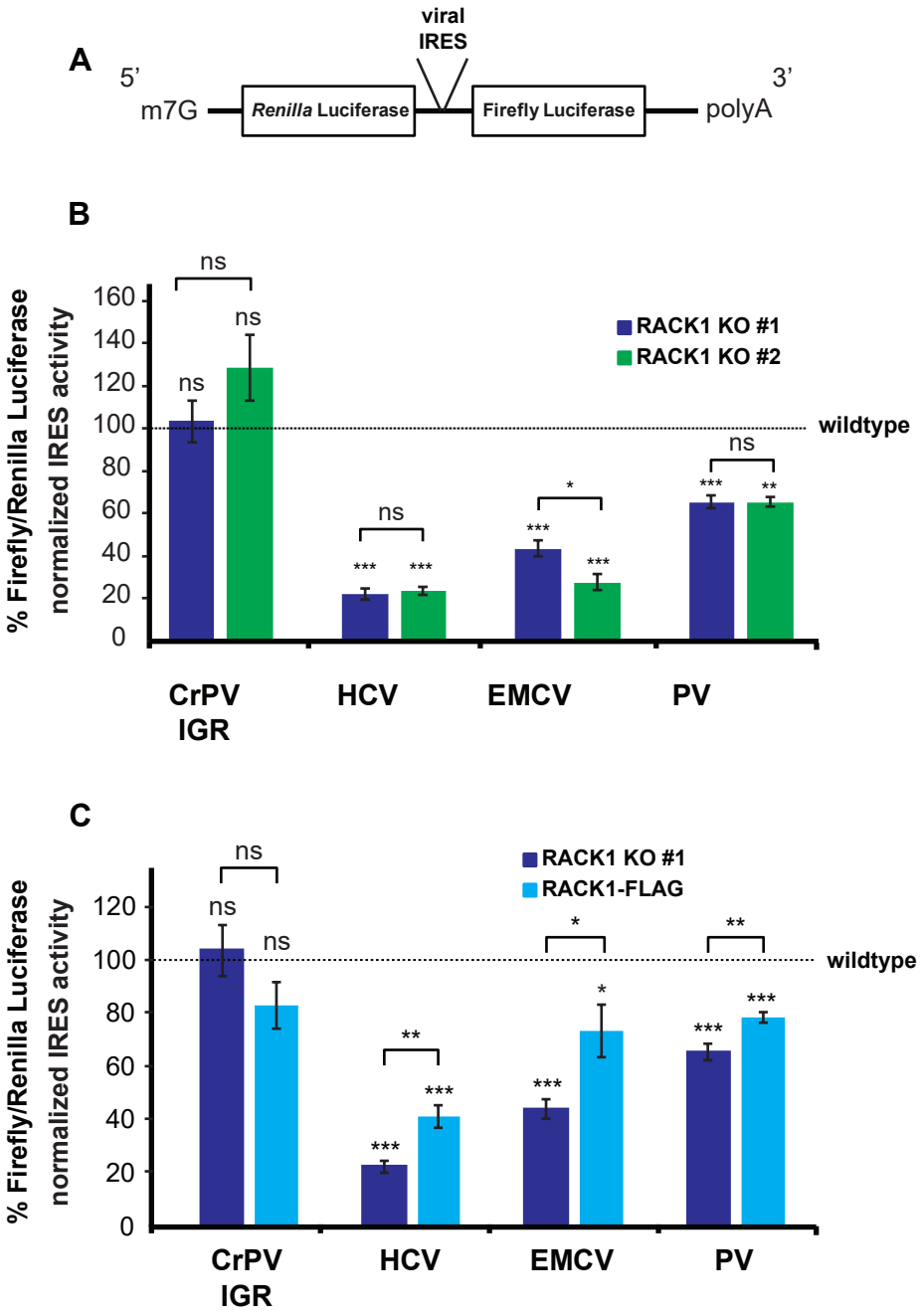

Figure 3

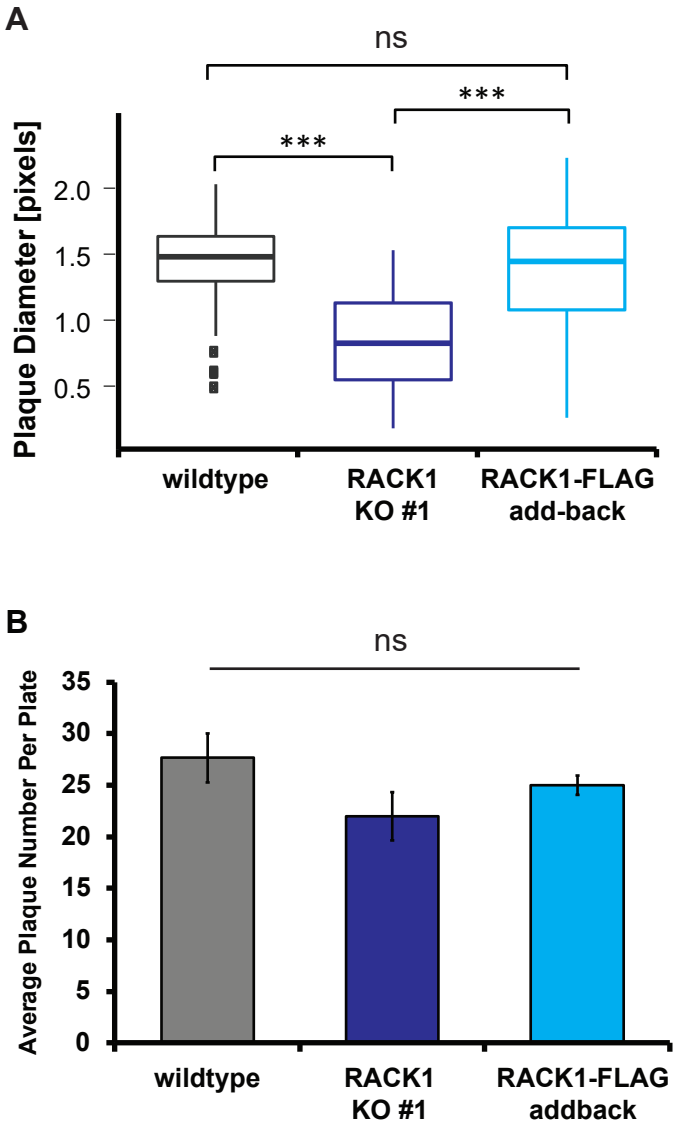

Figure 4

A

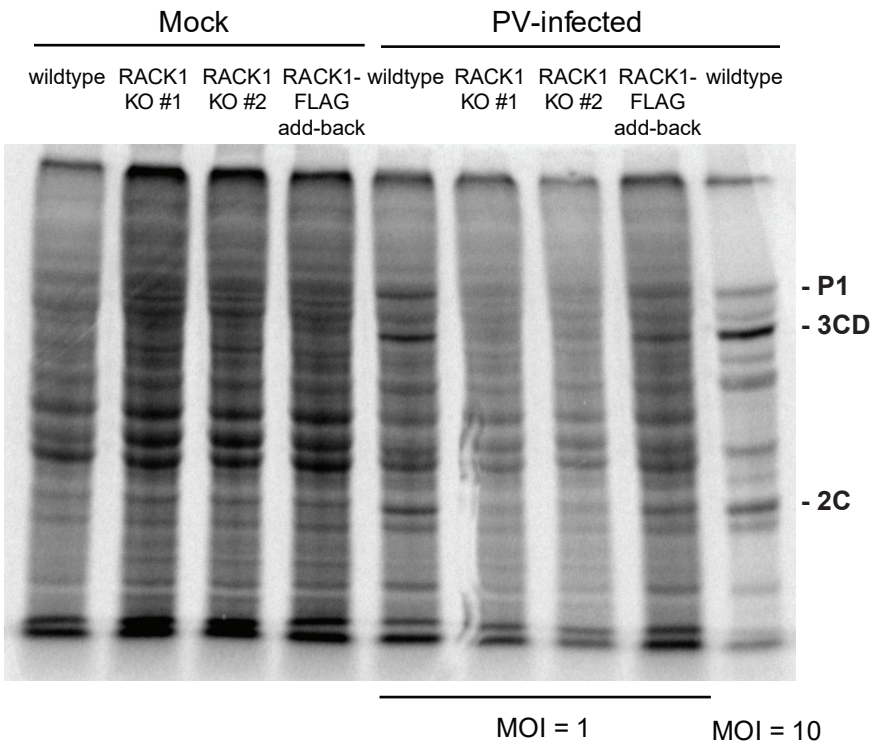

B